

Interspecific competition is thought to be a pervasive force in evolution (29, 30), and we suggest that the pattern we observe across Lakes Victoria and Tanganyika is likely due to competition between Nile perch and cichlid predators.

For nearly half a century, the robust pharyngeal jaws of cichlids, wrasses, and other pharyngognathous fishes have been considered a classic example of evolutionary innovation that opened up new niches through increased trophic flexibility (18). Although this is almost certainly correct, our results suggest that the innovation involves a major trade-off that severely limits the size of prey that can be eaten, facilitating competitive inferiority in predatory niches and extinction in the presence of a predatory invader lacking the innovation. The evolutionary innovation of pharyngognath is not a uniformly beneficial trait, but a specialization that can promote competitive exclusion and extinction depending on ecological context and community composition.

REFERENCES AND NOTES

1. E. Mayr, *Animal Species and Evolution* (Harvard Univ. Press Cambridge, MA, 1963).
2. S. B. Heard, D. L. Hauser, *Hist. Biol.* **10**, 151–173 (1995).
3. J. P. Hunter, *Trends Ecol. Evol.* **13**, 31–36 (1998).
4. R. Maia, D. R. Rubenstein, M. D. Shawkey, *Proc. Natl. Acad. Sci. U.S.A.* **110**, 10687–10692 (2013).
5. D. L. Rabosky, *PLOS ONE* **9**, e89543 (2014).
6. J. Cracraft, in *Evolutionary Innovations*, M. H. Nitecki, D. V. Nitecki, Eds. (Univ. of Chicago Press, Chicago, 1990), pp. 21–44.
7. G. J. Vermeij, *Biol. J. Linn. Soc. Lond.* **72**, 461–508 (2001).
8. G. J. Vermeij, *Paleobiology* **33**, 469–493 (2007).
9. G. J. Vermeij, *Evol. Ecol.* **26**, 357–373 (2012).
10. M. E. Alfaro, C. D. Brock, B. L. Banbury, P. C. Wainwright, *BMC Evol. Biol.* **9**, 255 (2009).
11. T. J. Givnish et al., *Evolution* **54**, 1915–1937 (2000).
12. S. A. Hodges, M. L. Arnold, *Proc. Biol. Sci.* **262**, 343–348 (1995).
13. D. Schluter, *The Ecology of Adaptive Radiation* (Oxford Univ. Press, Oxford, 2000).
14. D. Brawand et al., *Nature* **513**, 375–381 (2014).
15. C. Mitter, B. Farrell, B. Wiegmann, *Am. Nat.* **132**, 107–128 (1988).
16. D. J. Futuyma, G. Moreno, *Annu. Rev. Ecol. Syst.* **19**, 207–233 (1988).
17. T. J. Givnish, in *Evolution on Islands*, P. Grant, Ed. (Oxford Univ. Press, Oxford, 1998), pp. 281–304.
18. K. F. Liem, *Syst. Biol.* **22**, 425–441 (1973).
19. P. C. Wainwright, *J. Zool.* **213**, 283–297 (1987).
20. P. C. Wainwright et al., *Syst. Biol.* **61**, 1001–1027 (2012).
21. P. H. Greenwood, *The Haplochromine Fishes of the East African Lakes: Collected Papers on Their Taxonomy, Biology and Evolution* (Kraus International Publications, Munich, 1981).
22. O. Seehausen, *Proc. Biol. Sci.* **273**, 1987–1998 (2006).
23. F. Witte et al., *Environ. Biol. Fishes* **34**, 1–28 (1992).
24. G. W. Coulter, J.-J. Tiercelin, *Lake Tanganyika and Its Life* (Oxford Univ. Press, Oxford, 1991).
25. Materials and methods are available as supplementary materials on Science Online.
26. M. J. P. Van Oijen, *Neth. J. Zool.* **32**, 336–363 (1981).
27. O. Seehausen, J. J. Van Alphen, F. Witte, *Science* **277**, 1808–1811 (1997).
28. J. C. van Rijssel, F. Witte, *Evol. Ecol.* **27**, 253–267 (2013).
29. D. W. Pfennig, K. S. Pfennig, *Evolution's Wedge: Competition and the Origins of Diversity* (Univ. of California Press, Berkeley, CA, 2012).
30. D. L. Rabosky, *Annu. Rev. Ecol. Syst.* **44**, 481–502 (2013).

ACKNOWLEDGMENTS

We thank R. Bireley, J. Clifton, L. DeMason, R. Robbins, D. Schumacher, W. Wong, O. Selz, A. Taverna, M. Kayeba, M. Haluna, and the Lake

Victoria Species Survival Program for facilitating access to live and preserved specimens; the Tanzania Fisheries Research Institute for support and the Tanzania Commission for Science and Technology for research permits to O.S.; and R. Grosberg, D. Schluter, T. Schoener, D. Strong, M. Turelli, and G. Vermeij for manuscript comments. Funding was provided by NSF grants IOS-0924489, DEB-0717009, and DEB-061981 to P.C.W. and SNSF grant 31003A_144046 to O.S. R.Y.N. was supported by a Sloan Foundation grant to J. Eisen. All live animal protocols comply with UC Davis Guidelines for Animal Care and Use. Data are archived in Dryad.

SUPPLEMENTARY MATERIALS

www.sciencemag.org/content/350/6264/1077/suppl/DC1
Materials and Methods
Figs. S1 to S5
Tables S1 to S8
References (31–76)

8 March 2015; accepted 15 October 2015
10.1126/science.aab0800

CANCER IMMUNOTHERAPY

Anticancer immunotherapy by CTLA-4 blockade relies on the gut microbiota

Marie Vétizou,^{1,2,3} Jonathan M. Pitt,^{1,2,3} Romain Daillère,^{1,2,3} Patricia Lepage,⁴ Nadine Waldschmitt,⁵ Caroline Flament,^{1,2,6} Sylvie Rusakiewicz,^{1,2,6} Bertrand Routy,^{1,2,3,6} Maria P. Roberti,^{1,2,6} Connie P. M. Duong,^{1,2,6} Viichnou Poirier-Colame,^{1,2,6} Antoine Roux,^{1,2,7} Sonia Becharef,^{1,2,6} Silvia Formenti,⁸ Encouse Golden,⁸ Sascha Cording,⁹ Gerard Eberl,⁹ Andreas Schlitzer,¹⁰ Florent Ginhoux,¹⁰ Sridhar Mani,¹¹ Takahiro Yamazaki,^{1,2,6} Nicolas Jacquolot,^{1,2,3} David P. Enot,^{1,7,12} Marion Bérard,¹³ Jérôme Nigou,^{14,15} Paule Opolon,¹ Alexander Eggermont,^{1,2,16} Paul-Louis Woerther,¹⁷ Elisabeth Chachaty,¹⁷ Nathalie Chaput,^{1,18} Caroline Robert,^{1,16,19} Christina Mateus,^{1,16} Guido Kroemer,^{7,12,20,21,22} Didier Raoult,²³ Ivo Gomperts Boneca,^{24,25*} Franck Carbonnel,^{3,26*} Mathias Chamillard,^{5*} Laurence Zitvogel^{1,2,3,6†}

Antibodies targeting CTLA-4 have been successfully used as cancer immunotherapy. We find that the antitumor effects of CTLA-4 blockade depend on distinct *Bacteroides* species. In mice and patients, T cell responses specific for *B. thetaiotaomicron* or *B. fragilis* were associated with the efficacy of CTLA-4 blockade. Tumors in antibiotic-treated or germ-free mice did not respond to CTLA blockade. This defect was overcome by gavage with *B. fragilis*, by immunization with *B. fragilis* polysaccharides, or by adoptive transfer of *B. fragilis*-specific T cells. Fecal microbial transplantation from humans to mice confirmed that treatment of melanoma patients with antibodies against CTLA-4 favored the outgrowth of *B. fragilis* with anticancer properties. This study reveals a key role for *Bacteroidales* in the immunostimulatory effects of CTLA-4 blockade.

Ipilimumab is a fully human monoclonal antibody (Ab) directed against CTLA-4, a major negative regulator of T cell activation (1), approved in 2011 for improving the overall survival of patients with metastatic melanoma (MM) (2). However, blockade of CTLA-4 by ipilimumab often results in immune-related adverse events at sites that are exposed to commensal microorganisms, mostly the gut (3). Patients treated with ipilimumab develop Abs to components of the enteric flora (4). Therefore, given our previous findings for other cancer therapies (5), addressing the role of gut microbiota in the immunomodulatory effects of CTLA-4 blockade is crucial for the future development of immune checkpoint blockers in oncology.

We compared the relative therapeutic efficacy of the CTLA-4-specific 9D9 Ab against established MCA205 sarcomas in mice housed in specific pathogen-free (SPF) versus germ-free (GF) conditions. Tumor progression was controlled by Ab against CTLA-4 in SPF but not in GF mice (Fig. 1, A and B). Moreover, a combination of broad-spectrum antibiotics [ampicillin + colistin + strep-

tomylin (ACS)] (Fig. 1C), as well as imipenem alone (but not colistin) (Fig. 1C), compromised the antitumor effects of CTLA-4-specific Ab. These results, which suggest that the gut microbiota is required for the anticancer effects of CTLA-4 blockade, were confirmed in the Ret melanoma and the MC38 colon cancer models (fig. S1, A and B). In addition, in GF or ACS-treated mice, activation of splenic effector CD4⁺ T cells and tumor-infiltrating lymphocytes (TILs) induced by Ab against CTLA-4 was significantly decreased (Fig. 1, D and E, and fig. S1, C to E).

We next addressed the impact of the gut microbiota on the incidence and severity of intestinal lesions induced by CTLA-4 Ab treatment. A “subclinical colitis” dependent on the gut microbiota was observed at late time points (figs. S2 to S5). However, shortly (by 24 hours) after the first administration of CTLA-4 Ab, we observed increased cell death and proliferation of intestinal epithelial cells (IECs) residing in the ileum and colon, as shown by immunohistochemistry using Ab-cleaved caspase-3 and Ki67 Ab, respectively (Fig. 2A and fig. S6A). The CTLA-4 Ab-induced IEC proliferation

was absent in RegIII β -deficient mice (fig. S6A). Concomitantly, the transcription levels of *Il17a*, *Ifn γ* , *Ido1*, *type 1 Ifn*-related gene products and *Ctla4* (but not *Il6*), which indicate ongoing inflammatory processes, significantly increased by 24 hours in the distal ileum of CTLA-4 Ab-treated mice (fig. S6, B to D). Depletion of T cells, including intraepithelial lymphocytes (IELs) (by injection of Abs specific for CD4 and CD8), abolished the induction of IEC apoptosis by CTLA-4-specific Ab (Fig. 2A). When crypt-derived three-dimensional small intestinal enteroids (6) were exposed to Toll-like receptor (TLR) agonists (which act as microbial ligands in this assay) and subsequently admixed with IELs harvested from mice treated with Ab against CTLA-4 (but not isotype Ctl), IECs within the enteroids underwent apoptosis (Fig. 2B). Hence, CTLA-4 Ab compromises the homeostatic IEC-IEL equilibrium, favoring the apoptotic demise of IEC in the presence of microbial products.

To explore whether this T cell-dependent IEC death could induce perturbations of the microbiota composition, we performed high-throughput pyrosequencing of 16S ribosomal RNA (rRNA) gene amplicons of feces. The principal component analysis indicated that a single injection of CTLA-4 Ab sufficed to significantly affect the microbiome at the genus level (Fig. 2C). CTLA-4 blockade induced a rapid underrepresentation of both *Bacteroidales* and *Burkholderiales*, with a relative increase of *Clostridiales*, in

feces (Fig. 2C and table S1). Quantitative polymerase chain reaction (QPCR) analyses targeting the *Bacteroides* genus and species (spp.) in small intestine mucosa and feces contents showed a trend toward a decreased relative abundance of such bacteria in the feces, which contrasted with a relative enrichment in particular species [such as *B. thetaiotaomicron* (*Bt*) and *B. uniformis*] in the small intestine mucosa 24 to 48 hours after one CTLA-4 Ab injection (Fig. 2D and fig. S7). One of the most regulatory *Bacteroides* isolates, *B. fragilis* (*Bf*) (7–10), was detectable by PCR in colon mucosae

but was not significantly increased with CTLA-4 Ab (fig. S7).

Next, to establish a cause-and-effect relationship between the dominance of distinct *Bacteroides* spp. in the small intestine and the anticancer efficacy of CTLA-4 blockade, we recolonized ACS-treated and GF mice with several bacterial species associated with CTLA-4 Ab-treated intestinal mucosae as well as *Bf*. ACS-treated mice orally fed with *Bt*, *Bf*, *Burkholderia cepacia* (*Bc*), or the combination of *Bf* and *Bc*, recovered the anticancer response to CTLA-4 Ab, contrasting with all the other isolates that failed

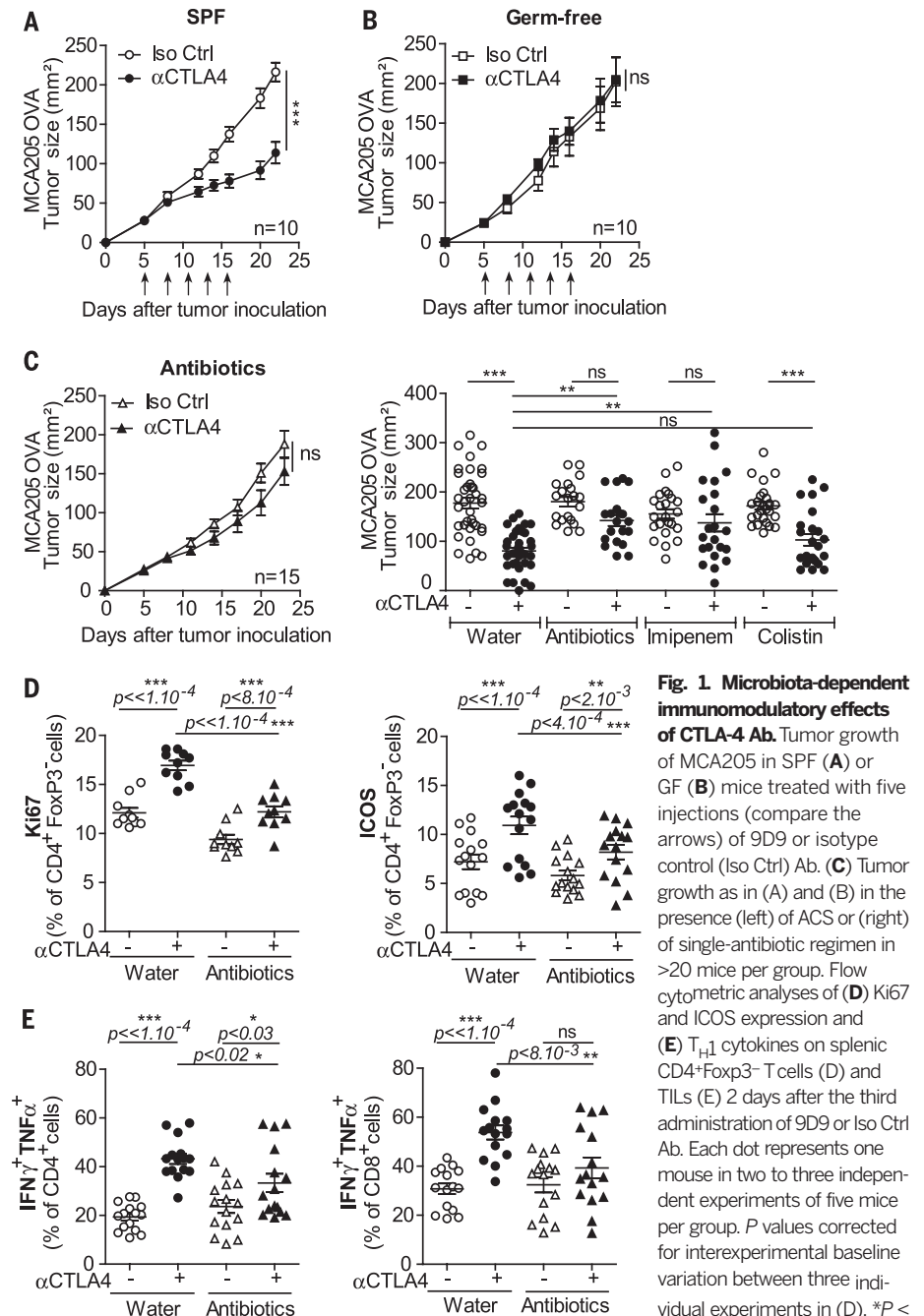


Fig. 1. Microbiota-dependent immunomodulatory effects of CTLA-4 Ab. Tumor growth of MCA205 in SPF (A) or GF (B) mice treated with five injections (compare the arrows) of 9D9 or isotype control (Iso Ctrl) Ab. (C) Tumor growth as in (A) and (B) in the presence (left) of ACS or (right) of single-antibiotic regimen in >20 mice per group. Flow cytometric analyses of (D) Ki67 and ICOS expression and (E) T_{H1} cytokines on splenic CD4⁺Foxp3⁻ T cells (D) and TILs (E) 2 days after the third administration of 9D9 or Iso Ctrl Ab. Each dot represents one mouse in two to three independent experiments of five mice per group. *P* values corrected for interexperimental baseline variation between three individual experiments in (D). **P* < 0.05, ***P* < 0.01, ****P* < 0.001; ns, not significant.

¹Institut de Cancérologie Gustave Roussy Cancer Campus (GRCC), 114 rue Edouard Vaillant, 94805 Villejuif, France. ²INSERM U1015, GRCC, Villejuif, France. ³University of Paris Sud XI, Kremlin-Bicêtre, France. ⁴Institut National de la Recherche Agronomique (INRA), Micalis-UMR1319, 78360 Jouy-en-Josas, France. ⁵University of Lille, CNRS, INSERM, Centre Hospitalier Régional Universitaire de Lille, Institut Pasteur de Lille, U1019, UMR 8204, Centre d'Infection et d'Immunité de Lille (CIIL), F-59000 Lille, France. ⁶Center of Clinical Investigations in Biotherapies of Cancer 1428, Villejuif, France. ⁷Université Paris Descartes, Sorbonne Paris Cité, Paris, France. ⁸Department of Radiation Oncology, New York University, New York, NY, USA. ⁹Microenvironment and Immunity Unit, Institut Pasteur, Paris, France. ¹⁰Singapore Immunology Network (SInG), Agency for Science, Technology and Research (A*STAR), Singapore, Singapore. ¹¹Department of Genetics and Department of Medicine, Albert Einstein College of Medicine, Bronx, NY 10461, USA. ¹²Metabolomics Platform, GRCC, Villejuif, France. ¹³Animagerie Centrale, Institut Pasteur, Paris, France. ¹⁴Centre National de la Recherche Scientifique, Institut de Pharmacologie et de Biologie Structurale (IPBS), Toulouse, France. ¹⁵Université de Toulouse, Université Paul Sabatier, IPBS, F-31077 Toulouse, France. ¹⁶Department of Medical Oncology, Institut Gustave Roussy, Villejuif, France. ¹⁷Service de microbiologie, GRCC, Villejuif, France. ¹⁸Laboratory of Immunomonitoring in Oncology, UMS 3655 CNRS/US 23 INSERM, GRCC, Villejuif, France. ¹⁹INSERM U981, GRCC, Villejuif, France. ²⁰INSERM U848, Villejuif, France. ²¹Equipe 11 Labellisée—Ligue Nationale contre le Cancer, Centre de Recherche des Cordeliers, INSERM U1138, Paris, France. ²²Pôle de Biologie, Hôpital Européen Georges Pompidou, Assistance Publique—Hôpitaux de Paris, France. ²³Unité des Rickettsies, Faculté de Médecine, Université de la Méditerranée, Marseille, France. ²⁴Institut Pasteur, Unit of Biology and Genetics of the Bacterial Cell Wall, Paris, France. ²⁵INSERM, Equipe Avenir, Paris, France. ²⁶Gastroenterology Department, Hôpital Bicêtre, Assistance Publique—Hôpitaux de Paris, Paris, France.

*These authors contributed equally to this work. †Corresponding author. E-mail: laurence.zitvogel@gustaveroussy.fr

to do so (table S2 and Fig. 3A). Similarly, oral feeding with *Bf*, which colonized the mucosal layer of GF mice (fig. S8) (11), induced T helper 1 (T_H1) immune responses in the tumor-draining lymph nodes and promoted the maturation of intratumoral dendritic cells (DCs), which culminated in the restoration of the therapeutic response of GF tumor bearers to CTLA-4 Ab (Fig. 3B and fig. S9, A and B).

We analyzed the dynamics of memory T cell responses directed against distinct bacterial species in mice and humans during CTLA-4 blockade. CD4⁺ T cells harvested from spleens of CTLA-4 Ab-treated mice (Fig. 3C) or from blood taken from individuals with MM or non-small cell lung carcinoma (NSCLC) patients after two administrations of ipilimumab (Fig. 3, D and E, and table S3) tended to recover a T_H1 phenotype (figs. S10 and S11). The functional relevance of such T cell responses for the anticancer activity

of CTLA-4 Ab was further demonstrated by the adoptive transfer of memory *Bf*-specific (but not *B. distasonis*-specific) T_H1 cells into GF or ACS-treated tumor bearers (Fig. 3F and fig. S12), which partially restored the efficacy of the immune checkpoint blocker.

The microbiota-dependent immunostimulatory effects induced by CTLA-4 blockade depended on the mobilization of lamina propria CD11b⁺ DC that can process zwitterionic polysaccharides (9) and then mount interleukin-12 (IL-12)-dependent cognate T_H1 immune responses against *Bf* capsular polysaccharides (figs. S13 and S14). However, they did not appear to result from TLR2/TLR4-mediated innate signaling (7, 8) in the context of a compromised gut tolerance (figs. S15 to S19).

To address the clinical relevance of these findings, we analyzed the composition of the gut microbiome before and after treatment with

ipilimumab in 25 individuals with MM (table S4). A clustering algorithm based on genus composition of the stools (12, 13) distinguished three clusters (Fig. 4A and table S5) with *Alloprevotella* or *Prevotella* driving cluster A and distinct *Bacteroides* spp. driving clusters B and C (Fig. 4B). During ipilimumab therapy, the proportions of MM patients falling into cluster C increased, at the expense of those belonging to cluster B (Fig. 4B and fig. S20A). We next performed fecal microbial transplantation of feces harvested from different MM patients from each cluster, 2 weeks before tumor inoculation into GF mice that were subsequently treated with anti-CTLA-4 Ab. Tumors growing in mice that had been transplanted with feces from cluster C patients markedly responded to CTLA-4 blockade, contrasting with absent anticancer effects in mice transplanted with cluster B-related feces (Fig. 4C). QPCR analyses revealed

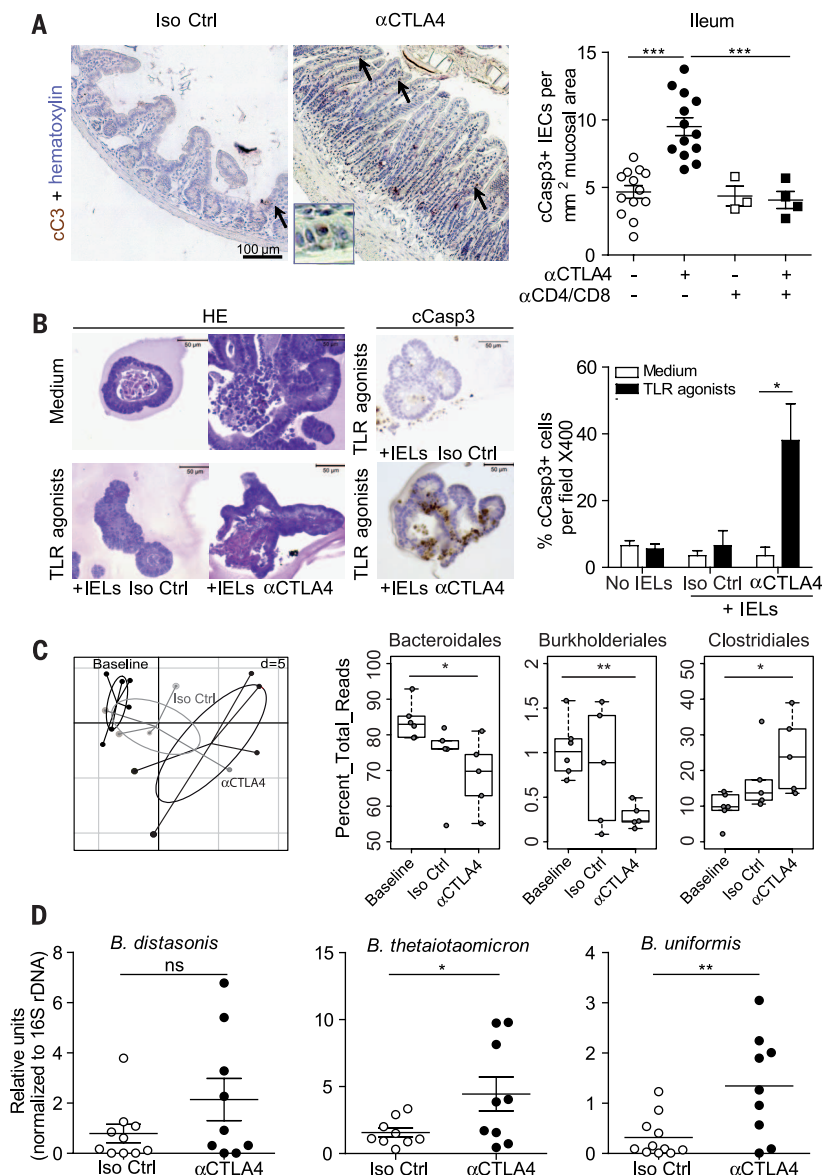
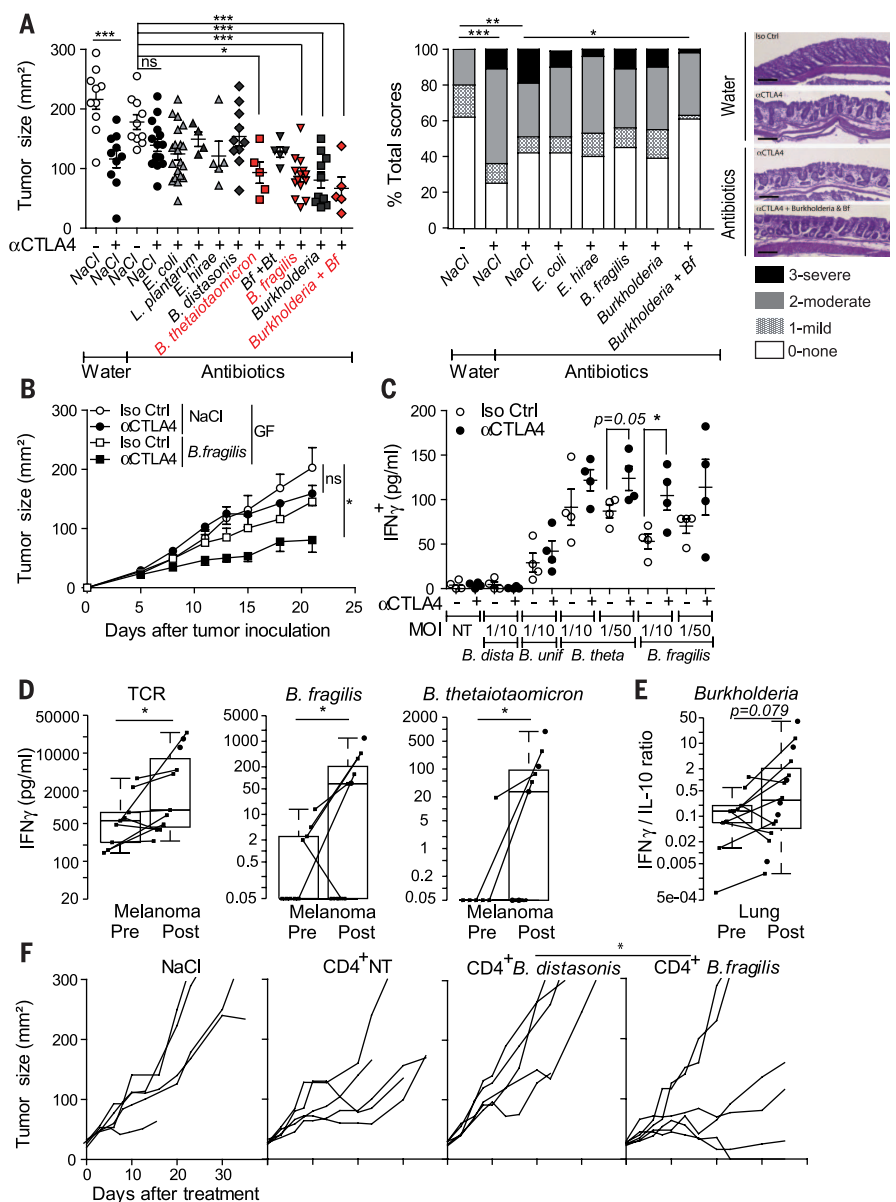


Fig. 2. IEC-IEL dialogue causes IEC apoptosis and intestinal dysbiosis after CTLA-4 Ab injection.

(A) (left) Representative micrograph pictures of distal ileum after staining with Ab-cleaved caspase 3 (cCasp3) Ab 24 hours after one injection of 9D9 (or Iso Ctrl) Ab in naïve mice with or without prior depletion of CD4⁺ and CD8⁺ T cells. Inset enlarged 18-fold. (Right) Concatenated data of two experiments. (B) (left) Representative micrographs of 3D enteroid cocultures stimulated (or not) with TLR agonists and incubated with IELs harvested from 9D9 (or Iso Ctrl) Ab-treated mice in hematoxylin and eosin (H&E), then (middle) stained with cCasp3-specific Ab. (Right) Data concatenated from two experiments counting the means \pm SEM percentages of apoptotic cells to organoid in 20 organoids. (C) Sequencing of 16S rRNA gene amplicons of feces from tumor bearers before and 48 hours after one administration of 9D9 or Iso Ctrl Ab. (Left) Principal component analysis (PCA) on a relative abundance matrix of genus repartition highlighting the clustering between baseline, Iso Ctrl Ab-, and 9D9 Ab-treated animals after one injection (five to six mice per group). Ellipses are presented around the centroids of the resulting three clusters. The first two components explain 34.41% of total variance (Component 1: 20.04%; Component 2: 14.35%) (Monte-Carlo test with 1000 replicates, $P = 0.0049$). (C) (right) Means \pm SEM of relative abundance for each three orders for five mice per group are shown. (D) QPCR analyses targeting three distinct *Bacteroides* spp. in ileal mucosae performed 24 to 48 hours after Ab introduction. Results are represented as $2^{-\Delta\Delta Ct} \times 10^3$, normalized to 16S rDNA and to the basal time point (before treatment). Each dot represents one mouse in two gathered experiments. * $P < 0.05$; ** $P < 0.01$; *** $P < 0.001$; ns, not significant.

Fig. 3. Memory T cell responses against *Bt* and *Bf* and anticancer efficacy of CTLA-4 blockade. (A and B) Tumoricidal effects of *Bf*, *Bt*, and/or *B. cepacia* (*Bc*) administered by oral feeding of ACS-treated or GF mice (also refer to fig. S8A). (A)

(left) Tumor sizes at day 15 after 9D9 or Iso Ctrl Ab treatment are depicted. Each dot represents one tumor, and graphs depict two to three experiments of five mice per group. (Middle) Histopathological score of colonic mucosae in ACS-treated tumor bearers receiving 9D9 Ab after oral gavage with various bacterial strains, assessed on H&E-stained colons monitoring microscopic lesions as described in materials and methods at day 20 after treatment in five animals per group on at least six independent areas. (Right) Representative micrographs are shown; scale bar, 100 μ m. (B) Tumoricidal effects of *Bf* in GF mice as indicated. (C to E) Recall responses of CD4⁺ T cells in mice and patients to various bacterial strains after CTLA-4 blockade. DCs loaded with bacteria of the indicated strain were incubated with CD4⁺ T cells, 2 days after three intraperitoneal (ip) CTLA-4 Ab in mice, and after at least two injections of ipilimumab (ipi) in patients. The graphs represent interferon- γ (IFN- γ) concentrations from coculture supernatants at 24 hours in mice (C) and 48 hours in MM patients (D). (E) IFN- γ /IL-10 ratios were monitored in DC-T cell cocultures of NSCLC patients at 48 hours. No cytokine release was observed in the absence of bacteria or T cells (fig. S11 with HV). Each dot represents one patient or mouse. Paired analyses are represented by linking dots pre- and post-ipi. (F) T cells harvested from spleens of mice exposed to CTLA-4 Ab and restimulated with *Bf* versus *B. distasonis* or bone marrow DCs alone (CD4⁺ NT) were infused intravenously in day 6 MCA205 tumor-bearing GF mice. A representative experiment containing five to six mice per group is shown. **P* < 0.05; ***P* < 0.01; ****P* < 0.001; ns, not significant.



that, although bacteria from the *Bacteroidales* order equally colonized the recipient murine intestine, stools from cluster C (but not A or B) individuals specifically facilitated the colonization of the immunogenic bacteria *Bf* and *Bt* (7–10, 14, 15) (Fig. 4D). Moreover, after CTLA-4 Ab therapy, only cluster C (not A or B) recipient mice had outgrowth of *Bf* (fig. S20B). Note that the fecal abundance of *Bf* (but not *B. distasonis* or *B. uniformis*) negatively correlated with tumor size after CTLA-4 blockade in cluster C-recipient mice (Fig. 4E and fig. S20C). Hence, ipilimumab can modify the abundance of immunogenic *Bacteroides* spp. in the gut, which in turn affects its anticancer efficacy.

Finally, intestinal reconstitution of ACS-treated animals with the combination of *Bf* and *Bc* did not increase but rather reduced histopathological signs of colitis induced by CTLA-4 blockade (Fig. 3A). This efficacy-toxicity uncoupling effect was not

achieved with vancomycin, which could boost the antitumor effects of CTLA-4 blockade (presumably by inducing the overrepresentation of *Bacteroidales* at the expense of *Clostridiales*) but worsened the histopathological score (fig. S21). In support of this notion, *Bf* maintained its regulatory properties in the context of CTLA-4 blockade (fig. S22) (7).

Hence, the efficacy of CTLA-4 blockade is influenced by the microbiota composition (*B. fragilis* and/or *B. theta* and/or *Burkholderiales*). The microbiota composition affects interleukin 12 (IL-12)-dependent T_H1 immune responses, which facilitate tumor control in mice and patients while sparing intestinal integrity. In accord with previous findings (16), colitis (observed in the context of IL-10 deficiency and CTLA-4 blockade) (fig. S17) could even antagonize anticancer efficacy. Several factors may dictate why such commensals could be suitable “anticancer

probiotics.” The geodistribution of *Bf* in the mucosal layer of the intestine (fig. S8) and its association with *Burkholderiales*—recognized through the pyrin-caspase-1 inflammasome (17) and synergizing with TLR2/TLR4 signaling pathways (fig. S15)—may account for the immunomodulatory effects of CTLA-4 Ab. Future investigations will determine whether a potential molecular mimicry between distinct commensals and/or pathobionts and tumor neoantigens could account for the toxicity and/or efficacy of immune checkpoint blockers. Prospective studies in MM and/or NSCLC may validate the relevance of the enterotypes described herein in the long-term efficacy of immune checkpoint blockers, with the aim of compensating cluster B-driven patients with live and immunogenic or recombinant *Bacteroides* spp. (18) or fecal microbial transplantation from cluster C-associated stools to improve their antitumor immune responses.

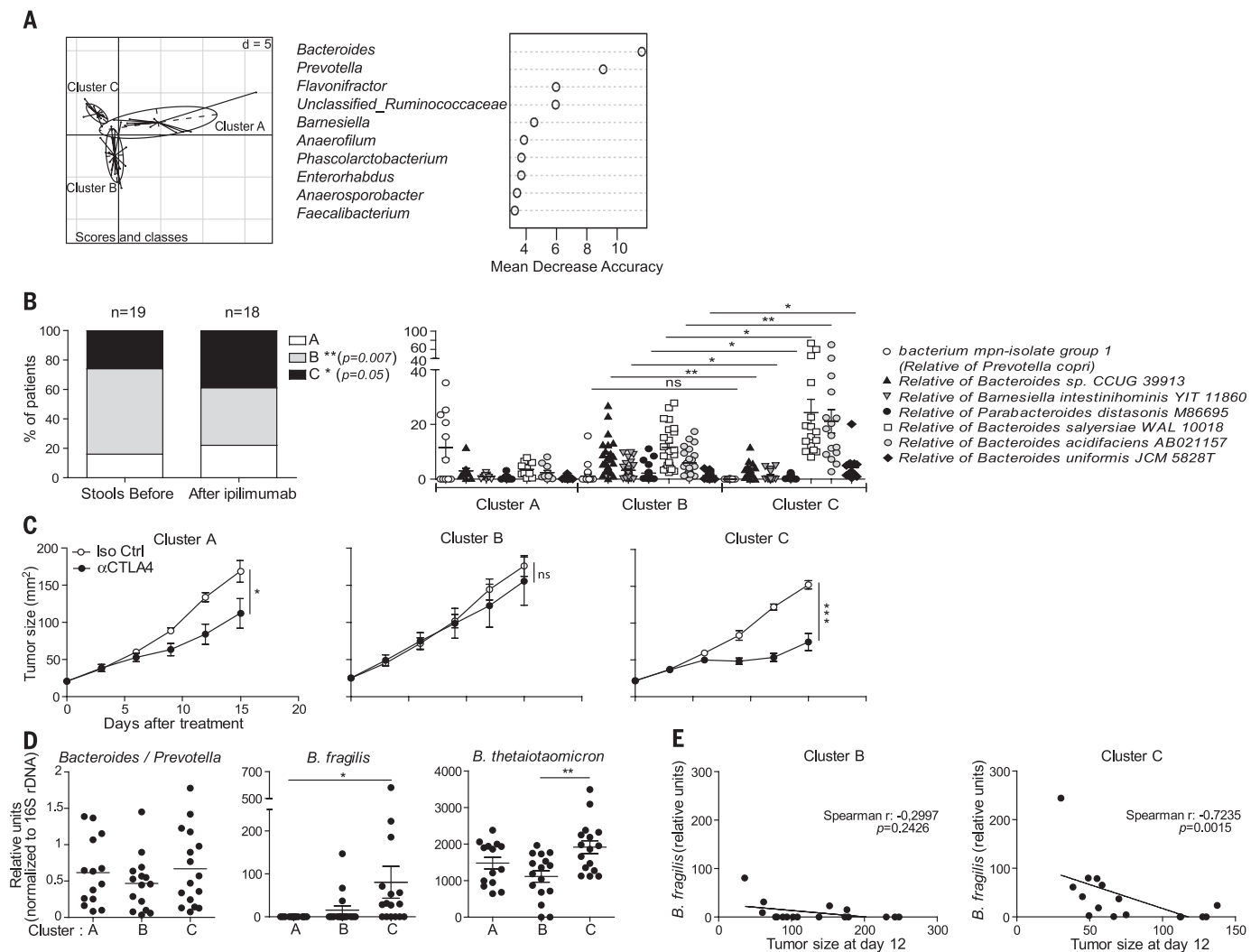


Fig. 4. Biological significance of ipilimumab-induced dysbiosis in patients.

The k means clustering algorithm was applied on the basis of genus composition before and during ipilimumab treatment in 25 MM patients, validated using the Calinski-Harabasz index (14), and showed good performance in recovering three clusters before and after therapy (interclass PCA); (A) (left) (Monte-Carlo test, $P = 0.000199$). (A) (right) Random Forest analysis was applied to decipher the main genera responsible for this significant clustering. (B) (right) The relative abundance of main *Bacteroides* spp. significantly differed between clusters B and C. (B) (left) The proportions of patients falling into each cluster were analyzed in a nonpaired manner before versus after ipi injections regardless of the time point (fig. S20A). (C) Fecal microbial transplantation after introduction of

ipilimumab from eight patients falling into each of the three clusters (stool selection for fecal microbial transplantation marked with an asterisk * in fig. S20A) into GF animals. One representative experiment out of three is shown with means \pm SEM of tumor sizes depicted for each cluster over time. (D) QPCR analyses of feces DNA of the recipient before (2 weeks postcolonization) and 2 weeks after ipi, targeting *Bacteroidales* and *Bacteroides* spp. Results are represented as $2^{-\Delta C_t} \times 10^3$, normalized to 16S rDNA. No significant difference in the relative abundance of *Bf* was detectable in the donors of cluster B versus C before colonization (not shown). (E) Spearman correlations between the amount of *Bf* in stools 15 days after treatment with 9D9 Ab and tumor sizes across cluster B- and C-recipient mice. * $P < 0.05$; ** $P < 0.01$; *** $P < 0.001$.

REFERENCES AND NOTES

1. K. S. Peggs, S. A. Quezada, A. J. Korman, J. P. Allison, *Curr. Opin. Immunol.* **18**, 206–213 (2006).
2. F. S. Hodi et al., *N. Engl. J. Med.* **363**, 711–723 (2010).
3. K. E. Beck et al., *J. Clin. Oncol.* **24**, 2283–2289 (2006).
4. D. Berman et al., *Cancer Immun.* **10**, 11 (2010).
5. S. Viaud et al., *Science* **342**, 971–976 (2013).
6. A. Rogoz, B. S. Reis, R. A. Karssemeijer, D. Mućica, *J. Immunol. Methods* **421**, 89–95 (2015).
7. S. Dasgupta, D. Erturk-Hasdemir, J. Ochoa-Reparaz, H. C. Reinecker, D. L. Kasper, *Cell Host Microbe* **15**, 413–423 (2014).
8. S. K. Mazmanian, C. H. Liu, A. O. Tzianabos, D. L. Kasper, *Cell* **122**, 107–118 (2005).
9. F. Stingele et al., *J. Immunol.* **172**, 1483–1490 (2004).
10. A. O. Tzianabos et al., *J. Biol. Chem.* **267**, 18230–18235 (1992).
11. J. Y. Huang, S. M. Lee, S. K. Mazmanian, *Anaerobe* **17**, 137–141 (2011).
12. M. Arumugam et al., *Nature* **473**, 174–180 (2011).

13. J. Qin et al., *Nature* **464**, 59–65 (2010).
14. A. Cebula et al., *Nature* **497**, 258–262 (2013).
15. J. L. Sonnenburg, C. T. Chen, J. I. Gordon, *PLoS Biol.* **4**, e413 (2006).
16. W. Lam et al., *Sci. Transl. Med.* **2**, 45ra59 (2010).
17. H. Xu et al., *Nature* **513**, 237–241 (2014).
18. M. Mimeo, A. C. Tucker, C. A. Voigt, T. K. Lu, *Cell Systems* **1**, 62–71 (2015).

ACKNOWLEDGMENTS

We are grateful to the staff of the animal facility of Gustave Roussy and Institut Pasteur. The data presented in this manuscript are tabulated in the main paper and in the supplementary materials. L.Z., M.V., and P.L. have filed patent application no. EP 14190167 that relates to the following: Methods and products for modulating microbiota composition for improving the efficacy of a cancer treatment with an immune checkpoint blocker. M.V. and J.M.P. were

supported by La Ligue contre le cancer and ARC, respectively. L.Z. received a special prize from the Swiss Bridge Foundation and ISREC. G.K. and L.Z. were supported by the Ligue Nationale contre le Cancer (Equipes labélisées), Agence Nationale pour la Recherche (ANR AUTOPH, ANR Emergence), European Commission (ArtForce), European Research Council Advanced Investigator Grant (to G.K.), Fondation pour la Recherche Médicale (FRM), Institut National du Cancer (INCa), Fondation de France, Cancéropôle Ile-de-France, Fondation Bettencourt-Schueller, Swiss Bridge Foundation, the LabEx Immuno-Oncology, the Institut national du cancer (SIRIC) Stratified Oncology Cell DNA Repair and Tumor Immune Elimination (SOCRATE); the SIRIC Cancer Research and Personalized Medicine (CARPEM), and the Paris Alliance of Cancer Research Institutes (PACRI). S.M. was supported by NIH (R01 CA161879, as Principal Investigator). M.C. was supported by the Fondation pour la Recherche Médicale, the Fondation ARC pour la recherche sur le cancer, and Institut Nationale du Cancer. N.W. is a recipient of a Postdoctoral Fellowship from the Agence

Nationale de la Recherche. A.S. was supported by BMSI YIG 2014. F.G. is supported by S1gN core funding. L.Z., M.C., and I.B.G. are all sponsored by Association pour la Recherche contre le Cancer (PGA120140200851). F.C. was supported by INCA-DGOS (GOLD H78008). N.C. was supported by INCA-DGOS (GOLD study; 2012-1-RT-14-IGR-01). L'Oreal awarded a prize to M.V. We are grateful to the staff of the animal facility of Gustave Roussy and Institut Pasteur. We thank P. Gonin, B. Ryyffel, T. Angélique, N. Chanthapathet, H. Li, and S. Zuberogoiita for technical help. DNA sequence reads from this

study have been submitted to the NCBI under the Bioproject IDPRJNA299112 and are available from the Sequence Read Archive (SRP Study accession SRP065109; run accession numbers SRR2758006, SRR2758031, SRR2758178, SRR2758179, SRR2758180, SRR2758181, SRR2768454, and SRR2768457.

SUPPLEMENTARY MATERIALS

www.sciencemag.org/content/350/6264/1079/suppl/DC1
Materials and Methods

Figs. S1 to S22
Tables S1 to S5
References (19–35)

3 April 2015; accepted 21 October 2015
Published online 5 November 2015;
10.1126/science.aad1329

CANCER IMMUNOTHERAPY

Commensal *Bifidobacterium* promotes antitumor immunity and facilitates anti-PD-L1 efficacy

Ayelet Sivan,^{1*} Leticia Corrales,^{1*} Nathaniel Hubert,² Jason B. Williams,¹ Keston Aquino-Michaels,³ Zachary M. Earley,² Franco W. Benyamin,¹ Yuk Man Lei,² Bana Jabri,² Maria-Luisa Alegre,² Eugene B. Chang,² Thomas F. Gajewski^{1,2,†}

T cell infiltration of solid tumors is associated with favorable patient outcomes, yet the mechanisms underlying variable immune responses between individuals are not well understood. One possible modulator could be the intestinal microbiota. We compared melanoma growth in mice harboring distinct commensal microbiota and observed differences in spontaneous antitumor immunity, which were eliminated upon cohousing or after fecal transfer. Sequencing of the 16S ribosomal RNA identified *Bifidobacterium* as associated with the antitumor effects. Oral administration of *Bifidobacterium* alone improved tumor control to the same degree as programmed cell death protein 1 ligand 1 (PD-L1)-specific antibody therapy (checkpoint blockade), and combination treatment nearly abolished tumor outgrowth. Augmented dendritic cell function leading to enhanced CD8⁺ T cell priming and accumulation in the tumor microenvironment mediated the effect. Our data suggest that manipulating the microbiota may modulate cancer immunotherapy.

Harnessing the host immune system constitutes a promising cancer therapeutic because of its potential to specifically target tumor cells although limiting harm to normal tissue. Enthusiasm has been fueled by recent clinical success, particularly with antibodies that block immune inhibitory pathways, specifically CTLA-4 and the axis between programmed cell death protein 1 (PD-1) and its ligand 1 (PD-L1) (1, 2). Clinical responses to these immunotherapies are more frequent in patients who show evidence of an endogenous T cell response ongoing in the tumor microenvironment before therapy (3–6). However, the mechanisms that govern the presence or absence of this phenotype are not well understood. Theoretical sources of interpatient heterogeneity include host germline genetic differences, variability in patterns of somatic alterations in tumor cells, and environmental differences.

The gut microbiota plays an important role in shaping systemic immune responses (7–9). In the cancer context, a role for intestinal microbiota in

mediating immune activation in response to chemotherapeutic agents has been demonstrated (10, 11). However, it is not known whether commensal microbiota influence spontaneous immune responses against tumors and thereby affect the therapeutic activity of immunotherapeutic interventions, such as anti-PD-1/PD-L1 monoclonal antibodies (mAbs).

To address this question, we compared subcutaneous B16.SIY melanoma growth in genetically similar C57BL/6 mice derived from two different mouse facilities, Jackson Laboratory (JAX) and Taconic Farms (TAC), which have been shown to differ in their commensal microbes (12). We found that JAX and TAC mice exhibited significant differences in B16.SIY melanoma growth rate, with tumors growing more aggressively in TAC mice (Fig. 1A). This difference was immune-mediated: Tumor-specific T cell responses (Fig. 1, B and C) and intratumoral CD8⁺ T cell accumulation (Fig. 1D) were significantly higher in JAX than in TAC mice. To begin to address whether this difference could be mediated by commensal microbiota, we cohoused JAX and TAC mice before tumor implantation. We found that cohousing ablated the differences in tumor growth (Fig. 1E) and immune responses (Fig. 1, F to H) between the two mouse populations, which suggested an environmental influence. Cohoused TAC

and JAX mice appeared to acquire the JAX phenotype, which suggested that JAX mice may be colonized by commensal microbes that dominantly facilitate antitumor immunity.

To directly test the role of commensal bacteria in regulating antitumor immunity, we transferred JAX or TAC fecal suspensions into TAC and JAX recipients by oral gavage before tumor implantation (fig. S1A). We found that prophylactic transfer of JAX fecal material, but not saline or TAC fecal material, into TAC recipients was sufficient to delay tumor growth (Fig. 2A) and to enhance induction and infiltration of tumor-specific CD8⁺ T cells (Fig. 2, B and C, and fig. S1B), which supported a microbe-derived effect. Reciprocal transfer of TAC fecal material into JAX recipients had a minimal effect on tumor growth rate and antitumor T cell responses (Fig. 2, A to C, and fig. S1B), consistent with the JAX-dominant effects observed upon cohousing.

To test whether manipulation of the microbial community could be effective as a therapy, we administered JAX fecal material alone or in combination with antibodies targeting PD-L1 (α PD-L1) to TAC mice bearing established tumors. Transfer of JAX fecal material alone resulted in significantly slower tumor growth (Fig. 2D), accompanied by increased tumor-specific T cell responses (Fig. 2E) and infiltration of antigen-specific T cells into the tumor (Fig. 2F), to the same degree as treatment with systemic α PD-L1 mAb. Combination treatment with both JAX fecal transfer and α PD-L1 mAb improved tumor control (Fig. 2D) and circulating tumor antigen-specific T cell responses (Fig. 2E), although there was little additive effect on accumulation of activated T cells within the tumor microenvironment (Fig. 2F). Consistent with these results, α PD-L1 therapy alone was significantly more efficacious in JAX mice compared with TAC mice (Fig. 2G), which paralleled improved antitumor T cell responses (fig. S1C). These data indicate that the commensal microbial composition can influence spontaneous antitumor immunity, as well as a response to immunotherapy with α PD-L1 mAb.

To identify specific bacteria associated with improved antitumor immune responses, we monitored the fecal bacterial content over time of mice that were subjected to administration of fecal permutations, using the 16S ribosomal RNA (rRNA) miSeq Illumina platform. Principal coordinate analysis revealed that fecal samples analyzed from TAC mice that received JAX fecal material gradually separated from samples obtained from sham- and TAC feces-inoculated TAC mice over time ($P = 0.001$ and $P = 0.003$, respectively, ANOSIM multivariate data analysis) and became similar

¹Department of Pathology, University of Chicago, Chicago, IL 60637, USA. ²Department of Medicine, University of Chicago, Chicago, IL 60637, USA. ³Section of Genetic Medicine, University of Chicago, Chicago, IL 60637, USA.

*These authors contributed equally to this work. †Corresponding author. E-mail: tgajewsk@medicine.bsd.uchicago.edu



Anticancer immunotherapy by CTLA-4 blockade relies on the gut microbiota

Marie Vétizou, Jonathan M. Pitt, Romain Daillère, Patricia Lepage, Nadine Waldschmitt, Caroline Flament, Sylvie Rusakiewicz, Bertrand Routy, Maria P. Roberti, Connie P. M. Duong, Vichnou Poirier-Colame, Antoine Roux, Sonia Becharef, Silvia Formenti, Encouse Golden, Sascha Cording, Gerard Eberl, Andreas Schlitzer, Florent Ginhoux, Sridhar Mani, Takahiro Yamazaki, Nicolas Jacquelot, David P. Enot, Marion Bérard, Jérôme Nigou, Paule Opolon, Alexander Eggermont, Paul-Louis Woerther, Elisabeth Chachaty, Nathalie Chaput, Caroline Robert, Christina Mateus, Guido Kroemer, Didier Raoult, Ivo Gomperts Boneca, Franck Carbonnel, Mathias Chamaillard and Laurence Zitvogel (November 5, 2015)

Science **350** (6264), 1079-1084. [doi: 10.1126/science.aad1329] originally published online November 5, 2015

Editor's Summary

Gut microbes affect immunotherapy

The unleashing of antitumor T cell responses has ushered in a new era of cancer treatment. Although these therapies can cause dramatic tumor regressions in some patients, many patients inexplicably see no benefit. Mice have been used in two studies to investigate what might be happening. Specific members of the gut microbiota influence the efficacy of this type of immunotherapy (see the Perspective by Snyder *et al.*). Vétizou *et al.* found that optimal responses to anticytotoxic T lymphocyte antigen blockade required specific *Bacteroides* spp. Similarly, Sivan *et al.* discovered that *Bifidobacterium* spp. enhanced the efficacy of antiprogrammed cell death ligand 1 therapy.

Science, this issue, p. 1079 and p. 1084; see also p. 1031

This copy is for your personal, non-commercial use only.

Article Tools Visit the online version of this article to access the personalization and article tools:
<http://science.sciencemag.org/content/350/6264/1079>

Permissions Obtain information about reproducing this article:
<http://www.sciencemag.org/about/permissions.dtl>

Science (print ISSN 0036-8075; online ISSN 1095-9203) is published weekly, except the last week in December, by the American Association for the Advancement of Science, 1200 New York Avenue NW, Washington, DC 20005. Copyright 2016 by the American Association for the Advancement of Science; all rights reserved. The title *Science* is a registered trademark of AAAS.